

## **General Disclaimer**

### **One or more of the Following Statements may affect this Document**

- This document has been reproduced from the best copy furnished by the organizational source. It is being released in the interest of making available as much information as possible.
- This document may contain data, which exceeds the sheet parameters. It was furnished in this condition by the organizational source and is the best copy available.
- This document may contain tone-on-tone or color graphs, charts and/or pictures, which have been reproduced in black and white.
- This document is paginated as submitted by the original source.
- Portions of this document are not fully legible due to the historical nature of some of the material. However, it is the best reproduction available from the original submission.



(NASA-CR-175350) RADAR INVESTIGATION OF  
ASTEROIDS Semiannual Status Report, 1 Jul.  
- 31 Dec. 1983 (Cornell Univ.) 14 p  
HC A02/MF A01

N84-17090

CSC 03B

Unclas

G3/91 00572

# **CORNELL UNIVERSITY**

*Center for Radiophysics and Space Research*

ITHACA, N. Y.

SEMI-ANNUAL STATUS REPORT

to the

NATIONAL AERONAUTICS AND SPACE ADMINISTRATION

under

NASA Grant NAGW-116

RADAR INVESTIGATION OF ASTEROIDS

July 1, 1983 - December 31, 1983

Principal Investigator: Professor Steven J. Ostro

CENTER FOR RADIOPHYSICS AND SPACE RESEARCH

CORNELL UNIVERSITY

ITHACA, NEW YORK 14853

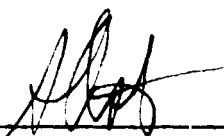
SEMI-ANNUAL STATUS REPORT

NASA Grant NAGW-116

July 1, 1983 - December 31, 1983

RADAR INVESTIGATION OF ASTEROIDS

Prepared January 1984



---

Professor Steven J. Ostro  
Principal Investigator

## TABLE OF CONTENTS

	<u>page</u>
I. SUMMARY OF PROGRESS . . . . .	1
New Radar Observations . . . . .	1
Highlights of Data Analysis . . . . .	<b>5</b>
II. FUNDING STATUS . . . . .	8
III. PUBLICATION OF RESULTS . . . . .	10

## I. SUMMARY OF PROGRESS

During the current report period, research supported under NASA Grant NAGW-116 proceeded as follows:

### New Radar Observations

The principal investigator conducted the initial radar observations of asteroids 80 Sappho, 356 Liguria, 694 Ekard, and 2340 Hathor. For each target, data were taken simultaneously in the same sense of circular polarization as transmitted (i.e., the "SC" sense) as well as in the opposite (OC) sense. [Estimates of the radar cross sections  $\sigma_{OC}$  and  $\sigma_{SC}$  provide estimates of the circular polarization ratio,  $\mu_C = \sigma_{SC}/\sigma_{OC}$ , and the geometric albedo,  $p = (1 + \mu_C)\hat{\sigma}_{OC}/4$ , where the normalized OC radar cross section is  $\hat{\sigma}_{OC} = \sigma_{OC}/A$ , with  $A$  the target's projected geometric area. The geometric albedo constitutes a first approximation to the target's Fresnel, normal-incidence, power-reflection coefficient,  $R$ .

Figure 1 shows dual-polarization echo power spectra for the main-belt objects Sappho, Liguria, and Ekard, which were easily detected. To maximize the signal-to-noise ratio, each spectrum has been smoothed using the indicated effective filter bandwidth (EFB). Standard errors applied to estimates of  $\mu_C$  correspond to the receiver noise in these EFB's.

ORIGINAL PAGE IS  
OF POOR QUALITY

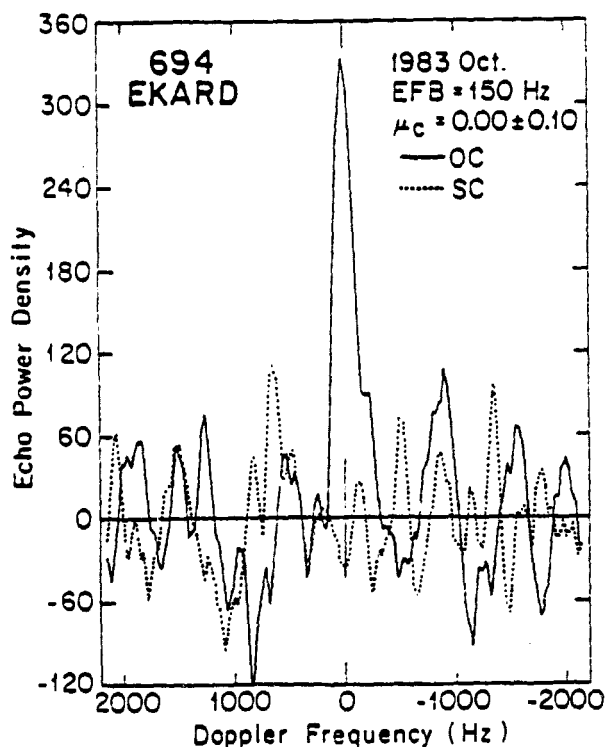
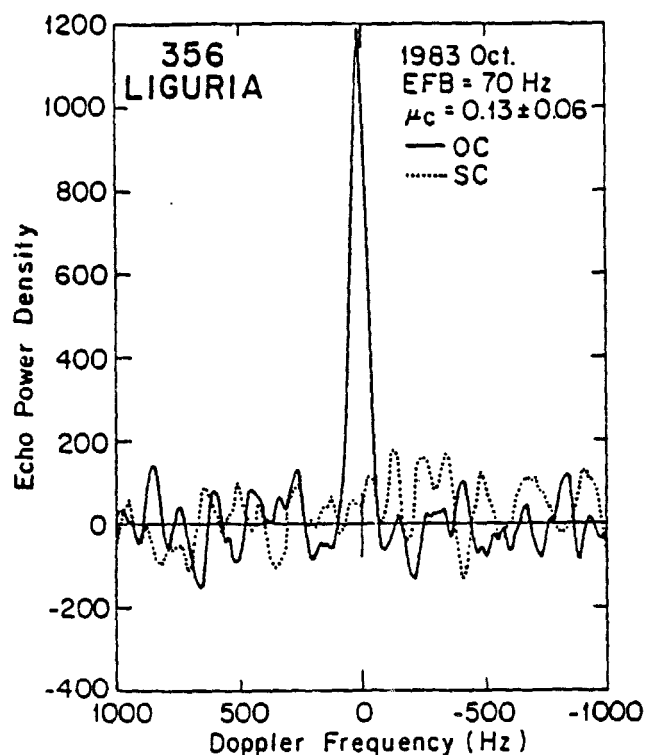
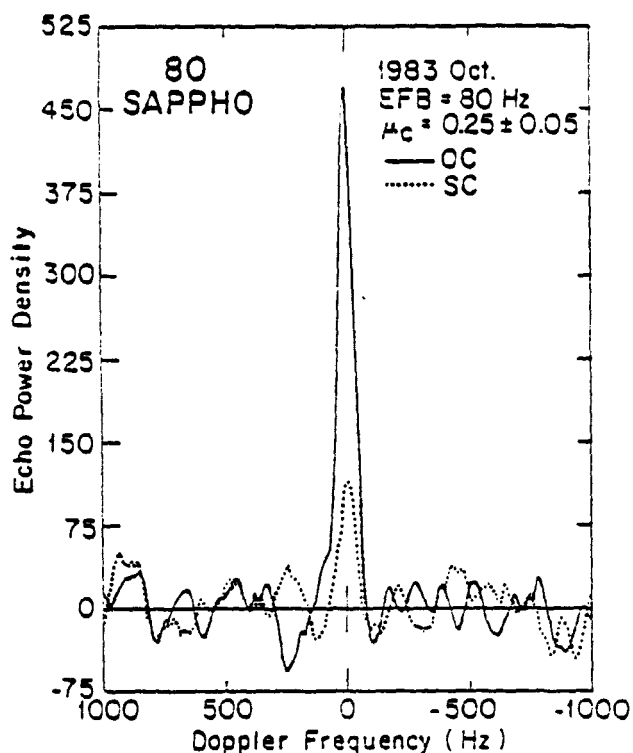


FIGURE 1

Average OC and SC radar echo power spectra, smoothed to a resolution of EFB Hz. Echo power density, in units of  $\text{km}^2$  of radar cross section per frequency resolution cell, is plotted against Doppler frequency. The central vertical bar represents plus and minus one standard deviation of the background noise.

The values of  $\mu_C$  obtained for Ekard and Liguria support earlier impressions that  $0 \leq \mu_C \leq 0.1$  for large C-type asteroids. On the other hand, Sappho's polarization ratio,  $\mu_C = 0.24 \pm 0.05$ , is the largest estimated for any main belt object and is more typical of tiny ( $\sim 1$  km) Earth-approaching asteroids (e.g., 1915 Quetzalcoatl, with  $\mu_C = 0.27 \pm 0.10$ ). The Sappho results comprise the first dual-polarization detection of radar echoes from an object with diameter between 40 and 95 km, as well as the first from a mainbelt object whose VIS/IR reflection spectrum suggests a surface mineralogy analogous to C3 carbonaceous chondrites.

Figure 2 shows unsmoothed OC spectra for Sappho and Liguria. The full echo bandwidths seem to be within about 10 Hz of 95 Hz and 90 Hz, respectively. When coupled with prior estimates of these objects' sizes and spin periods, these bandwidths suggest pole directions  $\sim 30^\circ$  and  $\sim 45^\circ$  from the radar line of sight.

ORIGINAL PAGE IS  
OF POOR QUALITY

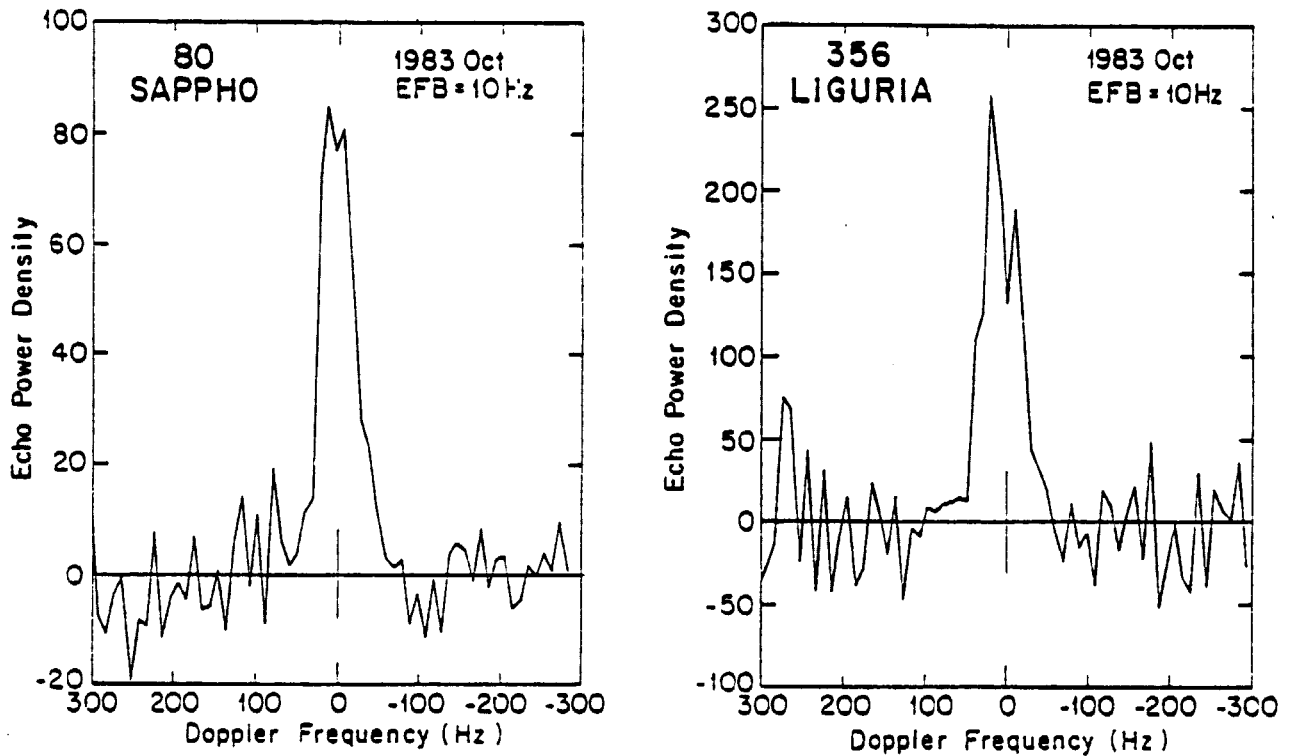


FIGURE 2

Average OC radar echo power spectra for Sappho and Liguria. Echo power density, in units of radar cross section per 10-Hz frequency resolution cell, is plotted against Doppler frequency. The central vertical bar represents plus and minus one standard deviation of the background noise.



### Highlights of Data Analysis

Radar observations last June of the peculiar object 2201 Oljato [comet-like orbit ( $a = 2.7$  AU,  $e = 0.71$ ,  $i = 2.5^\circ$ ); possible narrowband, cometary, UV emission features] reveal an unusual set of echo power spectra (Fig. 3). The albedo and polarization ratio remain fairly constant on June 13, 14, 16, and 17, but the bandwidths range from  $\sim 0.8$  Hz to  $\sim 1.4$  Hz and the spectral shapes vary dramatically. Echo characteristics within any one date's  $\sim 2.5$ -hr observation period do not fluctuate very much. The simplest interpretation of these results is that Oljato's shape is rather grotesque at meter to hectometer scales.

ORIGINAL PAGE IS  
OF POOR QUALITY

## 2201 OLJATO

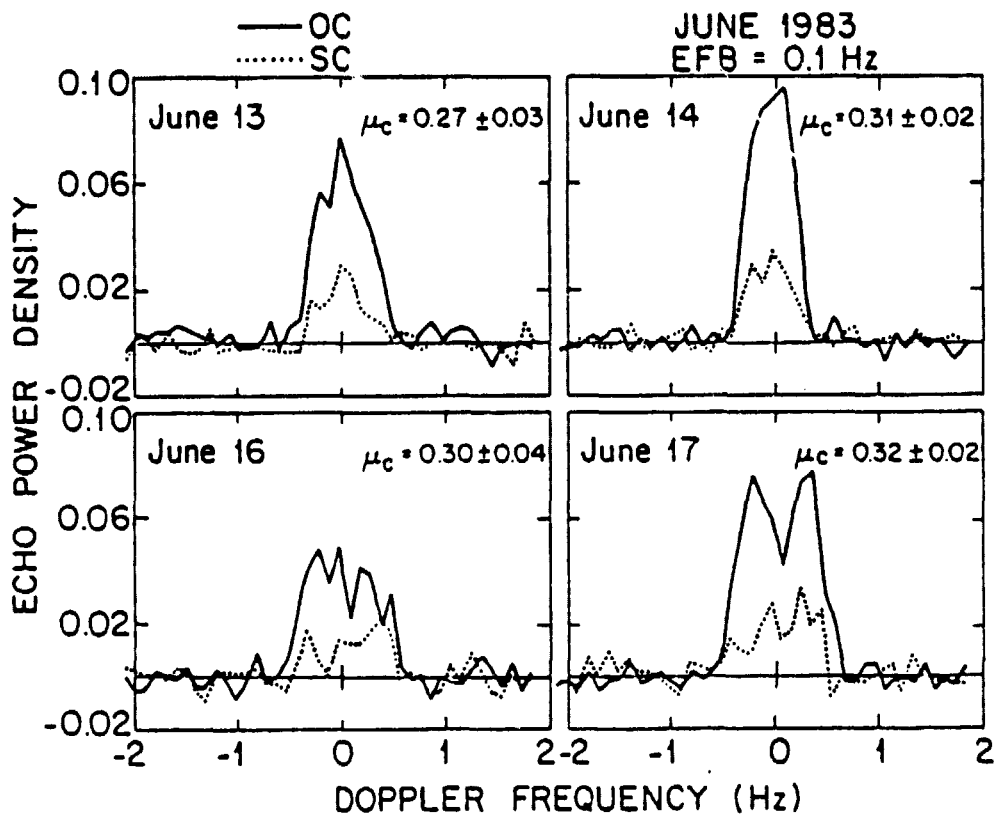


FIGURE 3

Average OC (solid curves) and SC (dotted curves) radar echo power spectra obtained for asteroid 2201 Oljato on four June 1983 dates. Echo power density, in units of  $\text{km}^2$  of radar cross section per 1-Hz resolution cell, is plotted against Doppler frequency. The standard deviation of the background noise was between 0.015 and 0.020  $\text{km}^2 \text{Hz}^{-1}$  on each night. Note the relatively high amplitude of the August 26 echo.

During the first year (1980-81) of the research supported under NASA Grant NAGW-116, it became clear that the power of radar constraints on asteroidal dimensions, spin vectors, and surface properties can be enhanced dramatically by photoelectric lightcurves acquired concurrently with the radar observations. If echo strength is adequate, observations at various rotational phases  $\phi$  can yield  $\sigma_{OC}$ ,  $\mu_C$ , and bandwidth as functions of  $\phi$ . Of course, if the rotation period  $P$  is unknown, nothing will be known about the extent of rotational phase coverage of the radar data. Even if  $P$  had been measured at a previous apparition, epochs of extreme light are unlikely to be predicted accurately, so the asteroid's rotational orientation as a function of time won't be known, and inferences from the radar data about target size and shape will suffer. Therefore, it is desirable that photoelectric lightcurves be obtained in tandem with radar observations.

In this context, the principal investigator has publicized (e.g., in the Minor Planet Bulletin) dates of planned asteroid radar observations, and has encouraged optical/infrared astronomers in the U.S. and abroad to conduct photometric and radiometric observations of radar-targeted objects. Partially as a result of these efforts, VIS/IR data were obtained in support of about 90% of the post-1981 radar experiments. The investigative power of combining data from several astronomical techniques has been demonstrated most recently in a paper, "Radar and Photoelectric Observations of Asteroid 2100 Ra-Shalom," by Ostro et al., soon to be submitted to Icarus.

During the current report period, the principal investigator finished a series of laboratory measurements at USGS and MIT of the radar-frequency electrical properties of particulate ( $\leq 40 \mu\text{m}$ ) metal-plus-silicate mixtures. By combining these measurements with radar albedo estimates, one can constrain the bulk density ( $d$ ) and metal weight fraction ( $w$ ) in a hypothetical asteroid regolith having the same particle-size distribution as the lab samples. For example, Fig. 4 shows contours of constant reflection coefficient ( $R$ ) and contours of constant porosity in the  $d, w$  plane. The bounds ( $0.05 \leq R \leq 0.3$ ) established on the reflection coefficient for 16 Psyche (an M-type object with the highest radar albedo of any radar-detected asteroid) require that: (i) if  $d < 1$ , then  $w > 0.6$ , so  $w$  is twice as large as the mean value for enstatite chondrites; (ii) if  $d > 1.5$ , then  $w$  can equal zero; (iii) if the surface is solid, then  $w$  must be less than 0.2 and an enstatite chondritic mineralogy is indicated for Psyche.

## II. FUNDING STATUS

Spending during the current report period was at the anticipated rate. A physics undergraduate, Anthony Ferro, has been hired on a part-time basis to assist the principal investigator with data analysis.

ORIGINAL PAGE IS  
OF POOR QUALITY

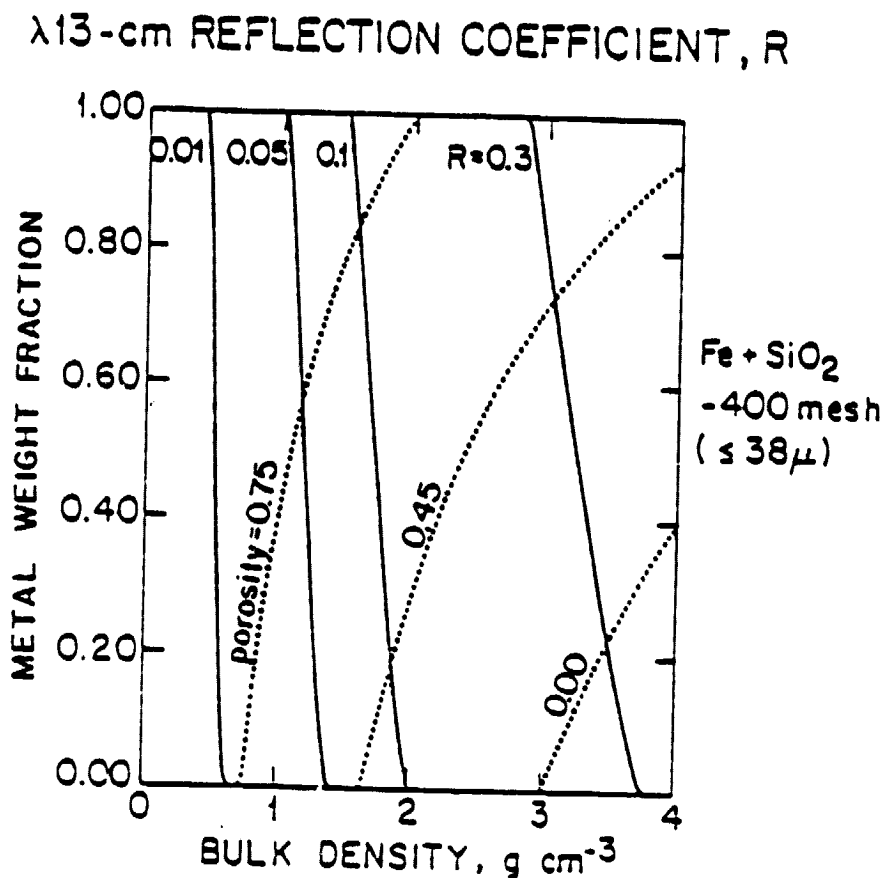


FIGURE 4

Constraints on the Fresnel, normal-incidence, power-reflection coefficient  $R$ , derived from laboratory measurements of the radar-frequency electrical properties of metal-plus-silica particulate mixtures.

### III. PUBLICATION OF RESULTS

During this period, results of the NASA-sponsored research were presented at the 15th Annual Meeting of the Division for Planetary Sciences of the American Astronomical Society (two abstracts appended). A paper (abstract appended) on the 1981 observations of 2100 Ra-Shalom will be submitted to Icarus in February, and a paper, "Radar Observations of Main-Belt Asteroids," is being prepared for submission to Science in May.